Theoret. chim. Acta (Berl.) 30, 9—30 (1973)


# Porphyrins XXVIII.* Extended Hückel Calculations on Metal Phthalocyanines and Tetrazaporphins

Arnold M. Schaffer, Martin Gouterman, and Ernest R. Davidson
Department of Chemistry, University of Washington, Seattle, Washington 98195

Received December 27, 1972

Extended Hückel (EH) calculations on Mg, Zn, Cu, Ni, Fe, Mn, and VO complexes of phthalocyanine and tetrazaporphin are reported and the results compared to similar calculations on porphyrins. The smaller ring size of phthalocyanine gives rise to a larger ligand field. The bridge nitrogen atoms give rise to $n-\pi^*$ transitions, which are probably in the region of the Soret band. In Ni, Co, Fe, and Mn there is strong mixing of the bridge N($2p_\sigma$) and metal $b_{2g}(d_{xy})$, which should affect the ligand field. Extra absorption bands observed in the near *uv* of NiPc and CoPc are attributed to $d_\pi \rightarrow \pi^*$ transitions. A general symmetrized EH program is reported that speeds calculations on large systems.

Für die Komplexverbindungen von Mg, Zn, Cu, Ni, Fe, Mn und Vo mit Phtalocyanin und Tetrazaporphin werden erweiterte Hückelrechnungen (EH) durchgeführt und die Ergebnisse mit ähnlichen Berechnungen an Porphyrinen verglichen. Die geringere Ringgröße des Phtalocyanins gibt Anlaß zu einem größeren Ligandenfeld. Das Brücken-Stickstoffatom gibt Anlaß zu $n$-$\pi^*$-Übergängen, die wahrscheinlich im Gebiet der Soret-Bande liegen. Beim Ni, Co, Fe und Mn tritt eine starke Mischung der Orbitale des Brückenstickstoff-Atoms N($2p_\sigma$) und $b_{2g}(d_{xy})$ auf, die das Ligandenfeld beeinflussen sollte. Die zusätzlichen Absorptionsbanden, die im nahen UV bei NiPc und CoPc beobachtet werden, werden $d_\pi \rightarrow \pi^*$-Übergängen zugeordnet. Ein allgemeines, symmetrisiertes EH-Programm wird mitgeteilt, das die Berechnung großer Systeme beschleunigt.

## Introduction

Previous papers in this series have reported extended Hückel (EH) calculations on a variety of porphyrins and related systems. Studies have been reported for porphyrin complexes with various first row transition metals [1–4], with alkali earth metals [5], and with Group IV metals [6], as well as EH calculations on free bases of porphin (P), tetrazaporphin (TAP), tetrabenzporphin (TBP), and phthalocyanine (Pc) [7]. This paper reports EH calculations on Mg and various first row transition metal complexes of phthalocyanine and tetrazaporphin. In tetrazaporphin the four methine bridge carbon atoms of porphin are replaced by nitrogen atoms. In phthalocyanine there is an additional perturbation of four benzo rings fused onto exo pyrole carbon atoms. The larger size of phthalocyanine required considerable computation time using the original EH programs, and a newer program was developed that is reported here. It allows for more atoms and up to three planes of symmetry – in contrast to the original program that allows only two planes [1, 4]. This paper focuses attention

* Paper XXVII. M. Gouterman, F. P. Schwarz, P. D. Smith, and D. Dolphin, J. chem. Physics, in press (1973).

on the similarities and contrasts among the porphyrin, tetrazaporphin, and phthalocyanine ring systems as shown by the EH calculations. In particular we consider effects on the ligand field and on electron densities.

Phthalocyanine molecules are similar in many ways but differ significantly from porphyrins. Although they do not occur naturally, since they were first synthesized and characterized by Linstead and co-workers [8, 9] they have found many scientific and commercial applications. Over 40 different metal complexes have been prepared, and phthalocyanines have found uses as dyes, catalysts, insulators, and passive $Q$-switches for lasers [10]. Their vapor properties have been studied [11, 12] as well as their photoconductive, semiconductive, and magnetic properties as solids [13]. The tetrazaporphins have not been widely studied since the early reports on their spectra [14] and methods of synthesis [15].

The early calculations on phthalocyanines used one of two approaches: the free electron gas model developed by Kuhn and co-workers [16] or simple molecular orbital theory [17]. The former has been extended by the "projected electron density method" to predict bond lengths as well as spectra [18]. SCMO-PPP theory was applied to phthalocyanine and tetrazaporphin sometime ago [19] and difficulties with the larger phthalocyanine system have been resolved more recently [20]. Linder and Rowlands [21] have correlated SCMO-CI calculations on the excited states of Mg phthalocyanine negative ions with MCD spectra.

While all the above calculations have only included $\pi$ electrons, there have been a few attempts made to investigate the interaction of the metal with the Pc ring. Ponomarev and Kubarev [23] empirically treated the effects of the metal in a simple Hückel MO calculation. As an aid in analyzing the ESR spectrum of CuPc, Chen *et al.* [24] used a limited EH model to consider the interaction of Cu with the inner 16-membered ring of phthalocyanine. Kramer and Klein [25] used the EH method to correlate the calculated charge density of Fe in FePc with X-ray photoelectron spectra. Recently Mathur and Singh [26] have carried out a limited EH treatment of several metal phthalocyanines, but their unreasonable results suggest some type of error. Recently Henriksson, Roos, and Sundbom [27] treated CuPc by the "peel" electron method. This takes account of the $40\pi$ electrons, metal $3d$, $4s$, $4p$ electrons, and the $8\sigma$ orbitals of the inner and bridge nitrogens. Unlike the other calculations that include the metal electrons, the peel method takes explicit account of two-electron interactions. The calculations reported here are the only ones that include all valence electrons of the whole molecule, but unlike the peel calculations, two electron interactions are not explicitly included.

## Symmetrized Extended Hückel Program

While some of the calculations reported here were done with a symmetrized EH program originally written by Zerner [1, 4], most were performed by a revised more efficient computational method. While the Zerner program can handle up to two planes of symmetry, the present program can handly up to three. Written

for the CDC 6400, the present program will handle many more orbitals. It would, however, require modification before it could be used on any other computer. In this section we review the approximations of the EH method and how they were incorporated into the present program.

In this version of self-consistent extended Hückel theory the basis set is assumed to be the minimum set of SCF atomic orbitals. The overlap between these orbitals, $\langle\phi_i|\phi_j\rangle$, is approximated by $\langle\varphi_i|\varphi_j\rangle$ where $\varphi_i$ is a Slater-type orbital

$$\varphi_i = Nr^{n-l-1}e^{-\zeta r} \times \text{spherical polynomial} \tag{1}$$

with $\zeta$ chosen so that $\varphi_i$ and $\phi_i$ give about the same overlap integrals at normal bond lengths. The Hückel operator is approximated by

$$\begin{aligned}\langle\phi_i|H|\phi_j\rangle &= \tfrac{1}{4}(\alpha_i+\alpha_j)(K_i+K_j)\langle\varphi_i|\varphi_j\rangle \; i\neq j\\ \langle\phi_i|H|\phi_i\rangle &= \alpha_i\,.\end{aligned} \tag{2}$$

The diagonal elements $\alpha_i$ are approximated by

$$\alpha_i = \alpha_i^0(1-|q_v|)+|q_v|\,\alpha_i^{\pm} \tag{3}$$

where $\alpha^+$ or $\alpha^-$ is used as $q_v \gtrless 0$ and where $q_v$ is the net charge from the Mulliken population on atom $v$ associated with orbital $i$. The free atom valence state ionization potential is used for the $\alpha_i^0$ of C, N, O, H while atomic orbital ionization potentials are used for the metals [4]; the corresponding ionic ionization potentials are used for $\alpha_i^{\pm}$. The empirical interaction constants $K_i$ were all chosen to be 1.89 in these calculations although the program allows different $K_i$ for each electron shell in each atom (but not for different azimuthal quantum numbers within a shell).

The actual calculations are carried out with some symmetry factorization. The program can handle up to three mirror planes at right angles. If $\phi_i$ is an atomic orbital, then a symmetry adapted group orbital $\phi_{i,\Gamma}$ may be defined as

$$\phi_{i,\Gamma} = 2^{-N_i}\prod_{\text{all mirror}}(1+\chi_\Gamma(\sigma)\,\sigma)\,\phi_i \tag{4}$$

where $N_i$ is the number of mirror planes containing $\phi_i$ and $\chi_\Gamma(\sigma)=\pm 1$ is the character of reflection $\sigma$ in the irreducible representation $\Gamma$. With this normalization, the non-vanishing $\phi_{i,\Gamma}$ reduce to

$$\phi_{i,\Gamma} = \Pi'(1+\chi_\Gamma(\sigma)\,\sigma)\,\phi_i \tag{5}$$

where the prime indicates that the product is over all planes not containing the atomic center associated with $\phi_i$.

The overlap matrix between group orbitals is approximated by

$$\begin{aligned}\langle\phi_{i,\Gamma}|\phi_{j,\Gamma}\rangle &= \langle\Pi'(1+\chi_\Gamma(\sigma)\,\sigma)\,\varphi_i|\Pi''(1+\chi_\Gamma(\sigma)\,\sigma)\,\varphi_j\rangle\\ &= 2^q\langle\varphi_i|\Pi'''(1+\chi_\Gamma(\sigma)\,\sigma)\,\varphi_j\rangle\end{aligned} \tag{6}$$

where $q$ is the number of planes in $\prod_\sigma'$ containing the atomic center of $\varphi_j$ plus the number of planes in $\prod_\sigma''$ containing the atomic center of $\varphi_i$ and $\prod_\sigma'''$ is a product over mirror planes not containing the atomic center of $\varphi_i$ or $\varphi_j$. This

reduces the formula for the overlap to the minimum number of unique integrals $\langle\varphi_i|\sigma\varphi_j\rangle$.

The Hückel matrix may be similarly simplified since

$$\langle\phi_i|H|\sigma\phi_j\rangle = \tfrac{1}{4}(\alpha_i+\alpha_j)(K_i+K_j)\langle\phi_i|\sigma\phi_j\rangle \tag{7}$$

(i.e. $K_j$ and $K_{\sigma(j)}$ are chosen equal as are $\alpha_j^0$ and $\alpha_{\sigma(j)}^0$, and $q_v$ and $q_{\sigma(v)}$). With this assumption,

$$\langle\phi_{i,\Gamma}|H|\phi_{j,\Gamma}\rangle = \tfrac{1}{4}(\alpha_i+\alpha_j)(K_i+K_j)\langle\phi_{i,\Gamma}|\phi_{j,\Gamma}\rangle \; i\neq j \tag{8}$$

and

$$\langle\phi_{i\Gamma}|H|\phi_{i\Gamma}\rangle = \alpha_i K_i\langle\phi_{i,\Gamma}|\phi_{i,\Gamma}\rangle + \alpha_i(1-K_i)\,2^{N_\sigma-N_i} \tag{9}$$

where $N_\sigma$ is the total number of mirror planes.

The charges $q_v$ are defined for the molecular orbitals $\psi_{i,\Gamma}$ and the orbital occupation numbers $n_i$ by the equations:

$$\begin{aligned}\psi_{i,\Gamma} &= \sum_j C_{j,i}^{\Gamma}\phi_{j,\Gamma} \equiv \Sigma\, Y_{j,i}\phi_j \\ q_v &= Z_v - \sum_{i\,\text{on}\,v}\left[\sum_j \varrho_{i,j}\langle\phi_j|\phi_i\rangle\right]\end{aligned} \tag{10}$$

where $Z_v$ is the core charge of atom $v$ and

$$\varrho_{ij} = \sum_k n_k Y_{ik} Y_{jk}\,. \tag{11}$$

This can be rearranged to

$$\begin{aligned}q_v &= Z_v - \sum_{i\,\text{on}\,v}\left[\sum_\Gamma\sum_j \varrho_{ij}^{\Gamma}\langle\phi_{i,\Gamma}|\phi_{j,\Gamma}\rangle\right] \\ \varrho_{ij}^{\Gamma} &= \sum_k n_k^{\Gamma} C_{i,k}^{\Gamma} C_{j,k}^{\Gamma}\,.\end{aligned}$$

Hence the Hückel matrix elements are computable from $\langle\phi_{i\Gamma}|\phi_{j\Gamma}\rangle$, and the individual overlap integrals $\langle\varphi_i|\varphi_j\rangle$ do not need to be retained after the reduced overlap elements are formed.

The program operates in a standard fashion with the Givens procedure as modified by Householder and Wilkinson [28] used to find the eigenvectors of the Hückel matrix after it is transformed to an orthogonal basis by a Schmidt transformation. The only non-standard algorithm is that involved in the evaluation of $\langle\varphi_i|\varphi_j\rangle$. Rather than use the formulae for each different overlap of STO's, an exact numerical integration is used [29]. This algorithm is based on the fact that the overlap integrals are separable in elliptical coordinates and the points and weights for each of the three one-dimensional integrals in that coordinate system are easily computed and rotated back into cartesian coordinates. Further efficiency is gained since the same set of points will work with all azimuthal quantum numbers. The overlap routine will handle principle quantum numbers up to 6 and angular momentum up to $l=3$.

## Geometry

Although there have been several recent reviews on the X-ray structures of porphyrins [30, 31], there has been no similar recent review on the X-ray structures of phthalocyanine. Very little was done following the original

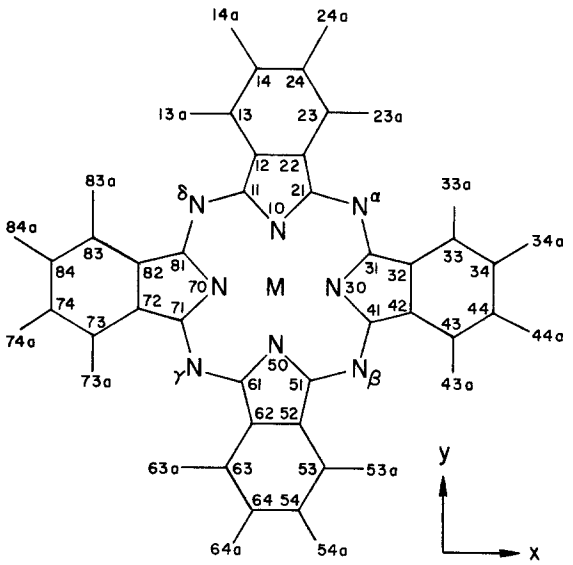


Fig. 1. Numbering scheme for phthalocyanine. The same numbers are used for TAP with the H atoms attached to 12, 22, 32, ... called 12a, 22a, 32a, ...

pioneering studies of Robertson and co-workers [32–34] until recently. In the last few years additional structures of phthalocyanines have been reported: the two polymorphs of PtPc [35], a neutron diffraction study of $H_2Pc$ [36], $MgPc \cdot H_2O \cdot (pyridine)_2$ [37], β-CuPc [38], $(Mn(III)Pc\ Pyridine)_2O$ [39], Sn(II)Pc [40], $Sn(IV)Cl_2Pc$ [41], a 4:1 amine complex between FePc and 4-methylpyridine [42], a 2:3 complex between ZnPc and *n*-hexylamine [43], and $Si[CH_3][OSi(C_2H_5)_3]Pc$ [44]. Only the structures of the Mg, Cu, and Sn(IV) compounds have been solved with an estimated standard deviation of less than 0.01 Å. An analysis of these structures leads to several general conclusions about the relation of phthalocyanine and porphyrin geometries, which we shall discuss in terms of the numbering scheme given in Fig. 1. We shall assume $D_{4h}$ symmetry.

(1) If the hole size is taken as the distance from the center to $N_\alpha$, phthalocyanines are on the average 0.065 Å smaller than the corresponding porphyrins.

(2) Concomitant with point (1) we find that for a given metal, the center to $N_{10}$ distance is 0.05 Å smaller in phthalocyanine than in porphyrin. (However for nickel this distance is 0.13 Å shorter, which may be exaggerated by experimental error.)

(3) The $C_{21}$–$N_\alpha$–$C_{31}$ bond angle is about 3° less in phthalocyanine, presumably a consequence of electron repulsion involving the lone pair on the trigonally hybridized nitrogen atom.

(4) The $C_{11}$–$C_{12}$ bond length in phthalocyanine is larger than in porphyrin, indicating less interaction between the inner 16-membered ring and the remaining electrons.

There are a number of structural reasons why the properties of metallophthalocyanines may differ from the corresponding porphyrins. These may

Table 1. Coordinates $(x, y)$ of tetrazaporphin and phthalocyanine in Å

| Atom | CuPc | CuTAP |
|---|---|---|
| Cu | (0, 0) | (0, 0) |
| $N_{10}$ | (0, 1.935) | (0, 1.935) |
| $C_{21}$ | (1.100, 2.745) | (1.100, 2.745) |
| $C_{22}$ | (0.701, 4.142) | (0.681, 4.142) |
| $C_{23}/H_{22a}$ | (1.407, 5.337) | (1.321, 5.002) |
| $H_{23a}$ | (2.487, 5.337) | – |
| $C_{24}$ | (0.709, 6.523) | – |
| $H_{24a}$ | (1.249, 7.458) | – |
| $N_\alpha$ | (2.376, 2.376) | (2.376, 2.376) |

Table 2. Distance (in Å) from plane of metal ($M$) and any fifth coordinating atom ($L$); distance from center of $N_{10}$

| | M(z) | L(z) | $N_{10}(y)$ |
|---|---|---|---|
| Mg[a] | 0.45 | – | 1.99 |
| VO | 0.48 | 2.11 (0) | 1.99 |
| Mn | 0 | – | 1.99 |
| Fe | 0 | [1.95 ($N_{pyr}$)][b] | 1.99 |
| Co | 0 | [1.95 ($N_{pyr}$)] | 1.90 |
| Ni | 0 | [1.95 ($N_{pyr}$)] | 1.90 |
| Cu | 0 | – | 1.935 |
| ZnPc | 0.448 | – | 1.99 |
| ZnTAP | 0 | – | 2.00 |

[a] Geometry of remaining atoms taken from X-ray structure [37], not from Table 1.
[b] Indicates the geometry used for the mono and bispyridine complexes of Fe and Ni and the monopyridinate complex of Co, which were calculated as discussed in the text.

include (i) presence of benzo groups, (ii) aza nitrogens at the bridge positions, (iii) different skeletal geometry, and (iv) different metal-nitrogen bond distances. In order to determine the influence of these last two factors, EH calculations were performed on various skeletal geometries for a given metal phthalocyanine. These calculations are discussed in more detail elsewhere [45]. In this paper, except for MgPc where we used a recent X-ray structure [37], we used the geometry of CuPc [38] as standard with the inner nitrogens moved out from the center to distances appropriate for the given metal. The structures used are given in Tables 1 and 2. For Fe, Co, and Ni, calculations were also done with pyridine as a ligand with geometry given in Table 2.

## Results

### *A.* Mg *and* Zn

Fig. 2 compares the MO energy levels of ZnP, ZnTBP, ZnTAP, and ZnPc. The effect on the $\pi$ MO's is as expected: $a_{2u}(\pi)$, $a_{1u}(\pi)$ and $e_g(\pi^*)$ of phthalocyanine are lowered by about 0.6, 0.3, and 0.5 eV respectively relative to

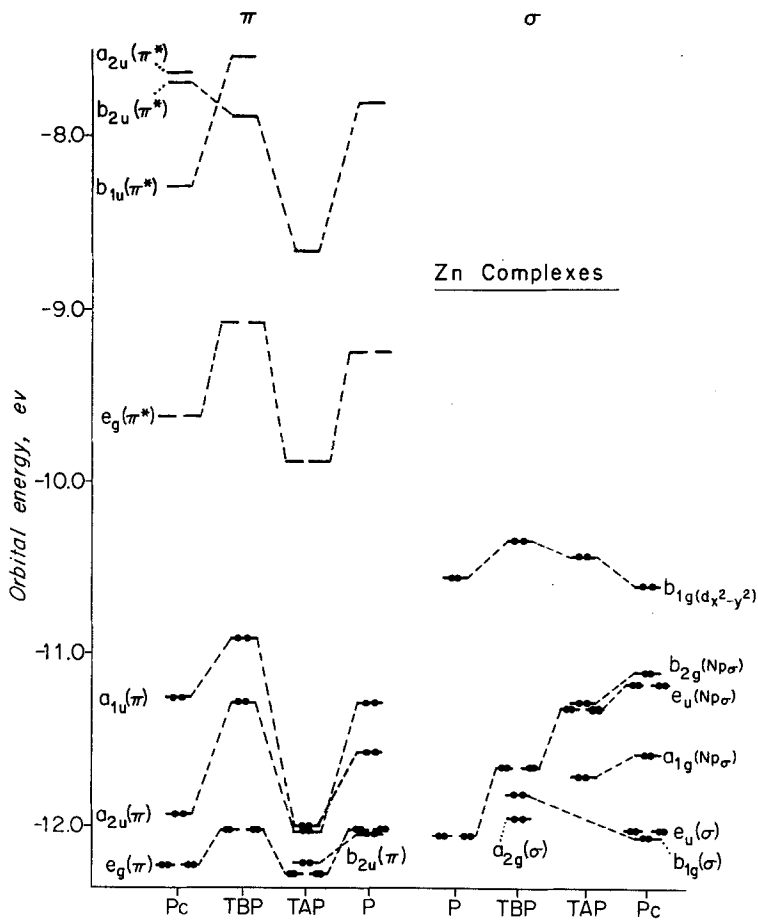


Fig. 2. Top filled and lowest empty $\pi$ and $\sigma$ MO's of ZnPc, ZnTBP, ZnTAP, and ZnP

tetrabenzporphin, while $a_{2u}(\pi)$, $a_{1u}(\pi)$, and $e_g(\pi^*)$ of tetrazaporphin are lowered by about 0.7, 0.4, and 0.6 eV respectively relative to porphin. More low energy $\pi^*$ orbitals appear in ZnPc and ZnTBP as compared to ZnTAP and ZnP. Also low energy filled $Np_\sigma$ orbitals, due to the bridge nitrogens appear in ZnTAP and ZnPc. Fig. 3 shows the orbitals of MgPc and MgTAP, which are essentially the same as the Zn complexes, except for a low energy empty $a_1(3p_z)$ at $\sim -7$ eV, slightly above the range of the diagram.

Are there any spectral effects due to these orbitals? Although there have been many studies of film and crystal spectra [46–48] as well as photoconductivity responses [49, 50], solution or vapor spectra are more useful for comparison with our calculations. Edwards' [12, 51] studies of phthalocyanine show for Mg and Zn five absorption bands assigned as $\pi\pi^*$: *Q*, *B*, *N*, *L*, and *C*, whose maxima are approximately 15200, 31300, 36400, 40800, and 47600 $cm^{-1}$ respectively. The spectra of tetrazaporphin have been less extensively studied [15, 52]. There are visible and Soret peaks at 17000 and 29500 $cm^{-1}$ with little study of the higher energy region. The $\pi\pi^*$ spectra are well accounted for

by SCMO-PPP calculations [19, 20]. The $Q$ band is relatively pure $a_{1u}(\pi)\rightarrow e_g(\pi^*)$, so there is some point to compare our EH calculated energy to the average of the lowest singlet and triplet transition in Pc, where the triplet is known [53]. Our calculated result ranges from 12800 to 13400 $cm^{-1}$ while the experimental range is 11800 to 12500 $cm^{-1}$. We predict the blue shift of the band in TAP.

The top filled $Np_\sigma$ orbitals in TAP and Pc may be expected to give rise to transitions, with $e_u(Np_\sigma)\rightarrow e_g(\pi^*)$ being allowed, $z$ polarized. The energy diagram of Fig. 2 suggests these transitions are at lower energy than the $Q$ bands, and in fact near *ir* absorption is observed in solid phase [48]. However, the fact that the $Q$ band fluoresces [11] is very strong evidence that it is the lowest excited singlet state in Mg and Zn complexes. The calculations of Henriksson and Sundbom [54] on free base phthalocyanine put the lowest energy $Np_\sigma\rightarrow e_g(\pi^*)$ in the Soret region. The EH calculations, while calibrated to fit $\pi\pi^*$ transitions, seem to generally underestimate transitions involving transfer of charge. We believe that underlying $Np_\sigma\rightarrow e_g(\pi^*)$ transitions are responsible for the broadening of the Soret region absorption observed in TAP and Pc as compared to P and TBP, in accord with the observations of Hochstrasser and Marzzacco [55] that underlying $n\pi^*$ transitions cause diffuseness in $\pi\pi^*$ bands.

There is other experimental evidence for the existence of at least one $n\pi^*$ transition between 15000 and 30000 $cm^{-1}$. In Mg triazatetrabenzporphin there is a weak but distinct band at $\sim$22000 $cm^{-1}$ [56]. This band could be very well due to a $n\pi^*$ transition, forbidden in a $D_{4h}$ molecule.

## *B.* Cu

Fig. 3 gives the MO diagram for CuPc and CuTAP. While the diagram shows $b_{1g}(d_{x^2-y^2})$ above $e_g(\pi^*)$, it is the former that contains the odd electron as shown by ESR [24, 57, 58]. If the odd electron is placed in $e_g(\pi^*)$, the EH calculation shows a strong reversal of their relative energies. While the diagram suggests that $b_{1g}(d_{x^2-y^2})\rightarrow e_g(\pi^*)$ should be low in energy, the observation of phosphorescence [53] shows this is not the case as does the peel calculation of Henriksson *et al.* [27].

From the ESR and magnetic properties [59, 60] the ligand field order has been established: $(d_{xy})^2<(d_\pi)^4<(d_{z^2})^2\ll(d_{x^2-y^2})^1$, which exactly matches calculated results. (The four lower energy $d$ orbitals are not shown in Fig. 3.) Because the $d_\pi$ energy is so low, it mixes little with $e_g(\pi^*)$ as shown in Table 3.

Using certain approximations, one can use the ESR [57, 58] and the magnetic susceptibility results [60] to calculate both the amount of metal delocalization and the ligand field splitting. Due to experimental uncertainty and the approximations involved, a range of values for these properties are obtained. The "experimental" $d_{xy}\rightarrow d_{x^2-y^2}$ energy separation varies from 26000 to 31000 $cm^{-1}$ while the $d_\pi\rightarrow d_{x^2-y^2}$ gap varies from 17000 to 29000 $cm^{-1}$. This compares to our calculated values of 33400 and 32500 $cm^{-1}$ respectively. We find (see Table 3) that the $b_{1g}(d_{x^2-y^2})$ orbital is only 28% localized on Cu while ESR results lead to a value $\sim$70% [57, 58]. From the ESR experiments $d_{xy}$ and $d_\pi$ are found to be $\sim$100% [57, 58] and $\sim$55% [58] localized which may be

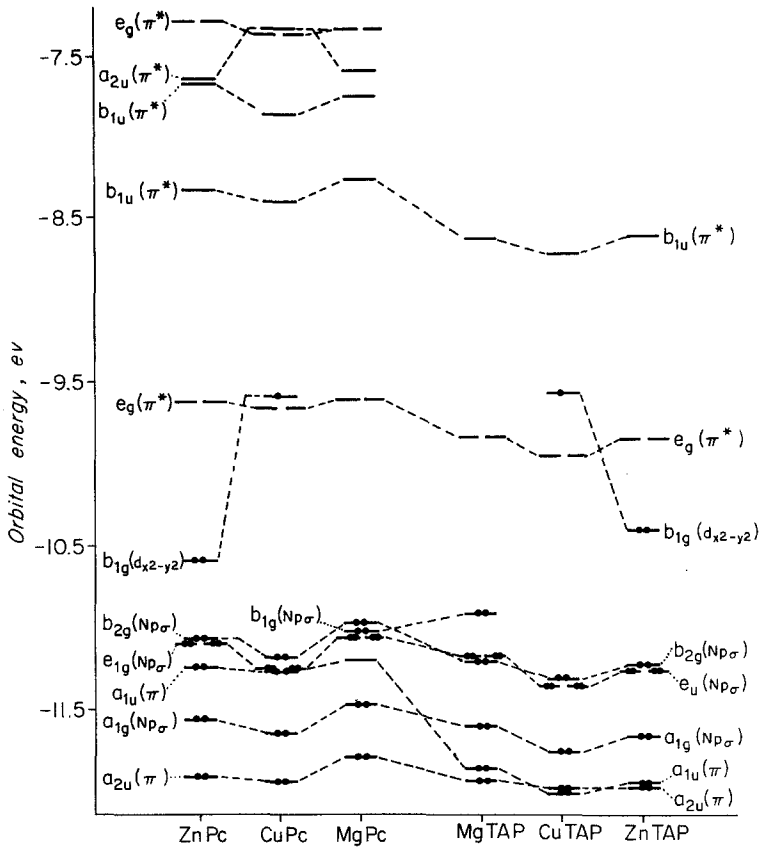


Fig. 3. Top filled and lowest empty MO's of ZnPc, CuPc, MgPc, ZnTAP, CuTAP, and ZnTAP

compared to our values of 92% and 40% respectively. Again our values are too low, but it should be noted that in the interpretation of the experimental ESR spectra, only interaction with the central nitrogens was considered. Henriksson *et al.* [27] found $b_{1g}(d_{x^2-y^2})$ to be 71% localized on the Cu.

The crystal structure of CuPc [38] indicates that the molecule is not perfectly $D_{4h}$. It is almost surely $D_{4h}$ in solution and vapor, but it is possible that crystal packing forces perturb the molecule slightly away from fourfold symmetry. To determine the effect of such a slight perturbation on the ligand field splitting, we used the geometry of Brown [38] directly; consequently, the angles between the pyrrole nitrogens and Cu are no longer 90%. In this configuration the $b_{1g}(d_{x^2-y^2})$ orbital is no longer pointing directly at the four pyrrole nitrogens. It thus has less antibonding character and as a result its energy is lowered $\sim 1.1$ eV and its metal composition increases to 60%. The effect on the $\pi$ orbitals is small although $e_g(\pi^*)$ is now split by 0.1 eV. This calculation indicates that even small distortions away from fourfold symmetry will have a large effect on ligand field splittings.

Table 3. Percent composition of top filled and lowest empty orbitals in phthalocyanines[a]

| | $a_{1u}(\pi)$ | | | |
|---|---|---|---|---|
| | $C_{11}$ | $C_{12}$ | $C_{13}$ | $C_{14}$ |
| Mg | 61.6 | 2.7 | 23.4 | 12.8 |
| Zn | 60.4 | 2.8 | 23.4 | 13.4 |
| Cu | 57.4 | 2.6 | 25.5 | 14.5 |
| Ni | 60.4 | 2.8 | 23.4 | 13.4 |
| Co | 60.5 | 2.8 | 23.3 | 13.4 |
| Fe | 59.9 | 2.5 | 24.0 | 13.6 |
| Mn | 59.3 | 2.3 | 24.7 | 13.7 |

| | $a_{2u}(\pi)$ | | | | | | |
|---|---|---|---|---|---|---|---|
| | $N_{10}$ | $C_{11}$ | $C_{12}$ | $C_{13}$ | $C_{14}$ | $N_\alpha$ | $4p_z$ |
| Mg[b] | 32.6 | 1.6 | 2.4 | 0.1 | 1.6 | 54.9 | 3.7 |
| Zn | 26.5 | 1.9 | 5.3 | 0.1 | 3.8 | 56.4 | 4.3 |
| Cu | 33.8 | 1.5 | 3.9 | 0.1 | 2.8 | 55.5 | 2.4 |
| Ni | 31.3 | 1.8 | 5.8 | 0.1 | 4.3 | 54.5 | 2.2 |
| Co | 26.9 | 2.1 | 7.8 | 0.2 | 6.0 | 54.6 | 2.4 |
| Fe | 33.2 | 1.3 | 3.3 | 0.1 | 2.2 | 58.2 | 1.7 |
| Mn | 35.6 | 0.9 | 2.5 | 0.1 | 1.8 | 57.9 | 1.2 |

| | $e_g(\pi^*)$ | | | | | | |
|---|---|---|---|---|---|---|---|
| | $N_{10}$ | $C_{11}$ | $C_{12}$ | $C_{13}$ | $C_{14}$ | $N_\alpha$ | $3d_\pi$ |
| Mg | 15.9 | 31.8 | 10.7 | 6.0 | 8.8 | 26.5 | — |
| Zn | 14.2 | 31.6 | 11.3 | 5.8 | 9.5 | 27.0 | <0.1 |
| Cu | 14.5 | 31.2 | 11.2 | 6.6 | 10.2 | 25.9 | 0.4 |
| Ni | 15.6 | 31.0 | 10.8 | 5.9 | 9.2 | 24.6 | 2.9 |
| Co | 15.6 | 29.8 | 10.7 | 5.6 | 9.0 | 24.6 | 4.7 |
| Fe | 13.9 | 30.3 | 11.2 | 5.5 | 9.2 | 27.3 | 2.6 |
| Mn | 13.5 | 30.1 | 10.9 | 5.4 | 9.1 | 26.9 | 4.1 |

| | $e_u(Np_\sigma)$ | | $a_{1g}(Np_\sigma)$ | | |
|---|---|---|---|---|---|
| $N_\alpha(2p_\sigma)$ | | $N_{10}(2p_\sigma)$ | $N_\alpha(2s)$ | $N_\alpha(2p_\sigma)$ | $N_{10}(2p_\sigma)$ |
| Mg | 60.0 | 21.2 | 7.3 | 68.1 | 9.3 |
| Zn | 59.3 | 18.8 | 8.0 | 68.6 | 7.5 |
| Cu | 59.0 | 20.6 | 7.7 | 67.8 | 8.9 |
| Ni | 60.5 | 19.8 | 8.1 | 69.2 | 8.4 |
| Co | 61.3 | 20.1 | 7.8 | 68.4 | 9.1 |
| Fe | 62.5 | 21.0 | 7.1 | 66.2 | 8.5 |
| Mn | 64.1 | 19.7 | 8.2 | 64.5 | 7.7 |

| | $b_{2g}(Np_\sigma)$ or $b_{2g}^*(d_{xy})$[c] | | |
|---|---|---|---|
| | $N_\alpha(2p_\sigma)$ | $N_{10}(2p_\sigma)$ | $3d_{xy}$ |
| Mg | 71.8 | 15.7 | — |
| Zn | 72.7 | 14.2 | 0.1 |
| Cu | 71.0 | 15.4 | 1.6 |
| Ni | 40.3 | 10.9 | 41.5 |
| Co | 30.2 | 8.7 | 54.8 |
| Fe | 38.6 | 9.9 | 42.5 |
| Mn | 26.1 | 7.9 | 60.1 |

Table 3 (Continued)

| | $b_{1g}(d_{x^2-y^2})$ | | | |
|---|---|---|---|---|
| | $N_\alpha(2p_\sigma)$ | $N_{10}(2s)$ | $N_{10}(2p_\sigma)$ | $3d_{x^2-y^2}$ |
| Mg[d] | 3.9 | 2.5 | 65.6 | — |
| Zn | 3.6 | 4.6 | 68.0 | 3.6 |
| Cu | 1.7 | 5.1 | 58.4 | 28.1 |
| Ni | 0.7 | 4.8 | 40.9 | 50.4 |
| Co | 0.6 | 4.8 | 39.8 | 53.2 |
| Fe | 1.0 | 3.5 | 41.8 | 49.7 |
| Mn | 0.9 | 3.6 | 41.0 | 51.1 |

| | $a_{1g}(d_{z^2})$ | | | $e_g(\pi)$ |
|---|---|---|---|---|
| | $N_\alpha(2p_\sigma)$ | $4s$ | $3d_{z^2}$ | $3d_\pi$ |
| Ni | 4.4 | 3.5 | 83.0 | 83.5 |
| Co | 3.8 | 4.2 | 87.0 | 83.9 |
| Fe | 8.3 | 4.4 | 73.1 | 85.1 |
| Mn | 6.3 | 5.8 | 81.8 | 84.1 |

| | $b_{2g}(d_{xy})$ | | |
|---|---|---|---|
| | $N_\alpha(2p_\sigma)$ | $N_{10}(2p_\sigma)$ | $3d_{xy}$ |
| Ni | 34.0 | 5.9 | 55.4 |
| Co | 44.9 | 8.1 | 40.9 |
| Fe | 36.0 | 5.1 | 55.3 |
| Mn | 47.2 | 7.4 | 36.4 |

[a] The total electron density for all $D_{4h}$ related atoms. For $\sigma$ orbitals and non-planar Mg and Zn $\pi$ orbitals, not all atomic orbitals with density are listed.
[b] $3p_z$ of MgPc.
[c] The $b_{2g}(Np_\sigma)$ orbital for Mg, Zn, and CuPc, otherwise $b^*_{2g}(d_{xy})$.
[d] The $b_{1g}(Np_\sigma)$ of MgPc.

## C. Ni

Fig. 4 gives the MO diagram for NiPc and NiTAP. The $b_{2g}(d_{xy})$ shows a curious behavior, which also occurs in Co, Fe, and Mn. It can be seen in the figures and in Tables 3 and 4. The $d_{xy}$ orbital, which is 96% pure in porphyrins, combines with the $b_{2g}(Np_\sigma)$ of the bridge nitrogens to give two orbitals. We call the higher energy orbital $b^*_{2g}(d_{xy})$ and the lower energy orbital $b_{2g}(d_{xy})$. Although our EH calculations usually overestimate delocalization of $d$ orbitals, we believe the different behavior of the $d_{xy}$ in TAP and Pc as compared to P and TBP due to the bridge nitrogens is real. As discussed below this delocalization may have effects on the magnetic properties and may also influence the absorption spectra.

There are two spectral phenomena in Ni complexes that should be noted. (i) There is no luminescence of Ni complexes of porphyrins [61] or phthalocyanines [53]. (ii) NiPc shows unusual absorption bands in the near UV at 35200, 42600, and 45900 $cm^{-1}$ [12]. The lack of luminescence suggests that the partly filled $d$ shell gives rise to transitions at lower energy than $\pi\pi^*$. Fielding

Table 4. Percent composition of the ligand field orbitals of tetrazaporphins[a]

| | $b_{1g}(d_{x^2-y^2})$ | | | |
|---|---|---|---|---|
| | $N_\alpha(2p_\sigma)$ | $N_{10}(2s)$ | $N_{10}(2p_\sigma)$ | $3d_{x^2-y^2}$ |
| Mg[b] | 3.3 | 4.3 | 75.4 | — |
| Zn | 2.8 | 2.8 | 76.1 | 3.0 |
| Cu | 1.3 | 3.2 | 59.9 | 28.2 |
| Ni | 0.6 | 4.8 | 41.6 | 50.2 |
| Co | 0.6 | 4.8 | 40.4 | 51.6 |
| Fe | 0.9 | 3.5 | 42.4 | 49.5 |
| VO | 0.7 | 4.5 | 24.9 | 35.7 |
| | $b^*_{2g}(d_{xy})$ | | | |
| | $N_\alpha(2p_\sigma)$ | $N_{10}(2p_\sigma)$ | $3d_{xy}$ | |
| Ni | 33.9 | 9.8 | 50.3 | |
| Co | 26.8 | 8.2 | 59.7 | |
| Fe | 34.8 | 9.4 | 48.6 | |
| | $b_{2g}(d_{xy})$ | | | |
| | $N_\alpha(2p_\sigma)$ | $N_{10}(2p_\sigma)$ | $3d_{xy}$ | |
| Ni | 41.8 | 8.0 | 45.8 | |
| Co | 49.6 | 9.5 | 35.8 | |
| Fe | 14.5 | 6.3 | 47.5 | |
| VO[c] | 6.2 | 3.2 | 86.8 | |
| | $a_{1g}(d_{z^2})$ | | | $e_g(d_\pi)$ |
| | $N_{10}(2p_\sigma)$ | $4s$ | $3d_{z^2}$ | $3d_\pi$ |
| Ni | 3.8 | 3.6 | 86.6 | 84.5 |
| Co | 3.7 | 4.3 | 88.0 | 82.0 |
| Fe | 8.3 | 4.8 | 78.3 | 84.9 |
| VO | 2.1 | 3.2 | 54.8 | 62.8 |

[a] The total electron density for all $D_{4h}$ related atoms.
[b] The $b_{1g}(Np_\sigma)$ of MgTAP.
[c] No $b^*_{2g}(d_{xy})$ orbital for VOTAP.

and MacKay [46] observe bands at $\sim 6400\,cm^{-1}$ in NiPc that they assign to $d-d$ transitions that would provide a radiationless path to the ground state. Our energy gap for $dd$ transitions in Ni is very large, which would suggest that any low energy $d-d$ transition must be a triplet. If there is no singlet below the singlet $\pi\pi^*$ then Ni complexes may show a weak fluorescence, as do Pd complexes [53, 62], a point that may have escaped experimental notice.

It has previously been suggested that the unusual absorption bands of NiPc in the UV region are $d\pi^*$ in origin [12]. There are two reasons why phthalocyanines have many more metal dependent bands than porphyrins: (1) additional delocalization of metal orbitals in phthalocyanines to give greater intensity to $d\pi^*$ transitions; (2) additional number of low lying empty $\pi^*$ orbitals to give a

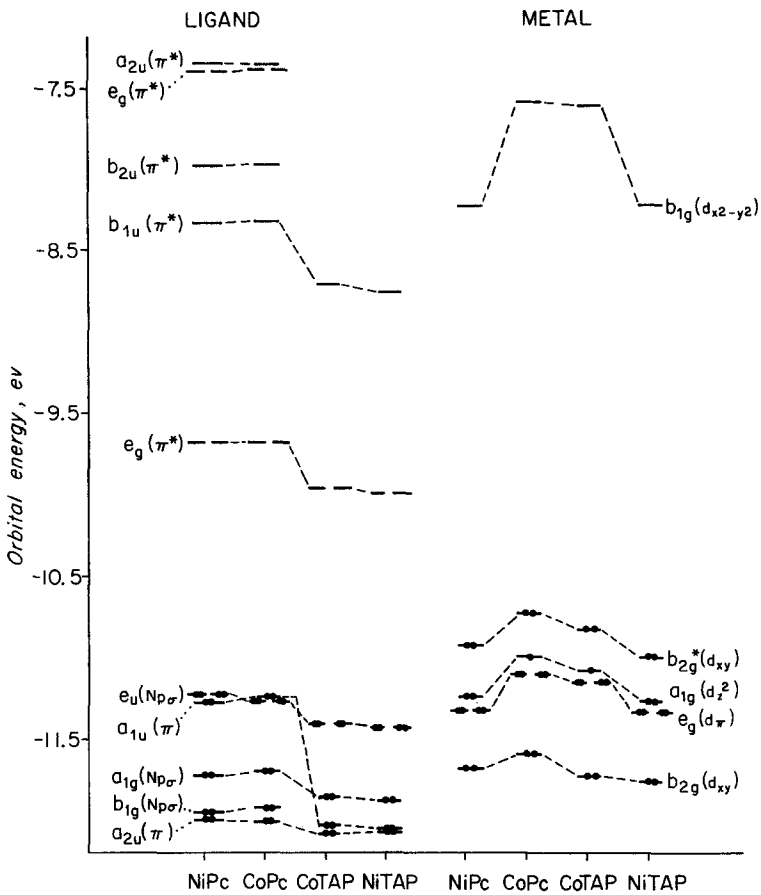


Fig. 4. Top filled and lowest empty MO's of NiPc, CoPc, NiTAP, and CoTAP. The ligand and metal orbitals are indicated separately. No fifth or sixth ligand on metal

greater number of allowed transitions. Table 5 lists the allowed $d\pi^*$ transitions with orbital energy differences of less than 45000 $cm^{-1}$ for Ni porphins [1] and phthalocyanines. Originally Edwards and Gouterman [12] assigned the NiPc near UV bands to $b_{2g}(d_{xy}) \rightarrow b_{1u}(\pi^*)$, since $d_{xy}$ is now considerably delocalized. However, this transition is $z$ polarized and even with the increased delocalization is probably too weak to explain the high intensity of these bands. Therefore, we propose that the three metal dependent bands of NiPc correspond to the three $d_\pi \rightarrow \pi^*$ transitions listed in Table 5. The fairly high intensity of these metal to phthalocyanine transitions is partly a consequence of the increased delocalization of the $d_\pi$ orbital in phthalocyanines compared to porphyrins. This in turn is a result of the decreased metal-nitrogen bond distance in phthalocyanines. For example, $d_\pi$ is an 83.5% metal orbital in NiPc with a Ni-N bond distance of 1.90 Å (Table 3), while in NiP $d_\pi$ is 90.0% localized for a Ni–N distance of 1.96 Å [1].

Table 5. Calculated energies ($cm^{-1}$) of allowed $d \rightarrow \pi^*$ transitions in NiP, NiPc, CoP, and CoPc[a]

| Transition | Polarization | NiP | NiPc(X) | CoP | CoPc(XII) |
|---|---|---|---|---|---|
| $b_{2g}^*(d_{xy}) \rightarrow b_{1u}(\pi^*)$ | $z$ | — | 20800 | — | 19500 |
| $b_{2g}(d_{xy}) \rightarrow b_{1u}(\pi^*)$ | $z$ | 25000 | 27000 | 23400 | 26500 |
| $a_{1g}(d_{z^2}) \rightarrow a_{2u}(\pi^*)$ | $z$ | — | 31200 | — | 29300 |
| $e_g(d_\pi) \rightarrow b_{1u}(\pi^*)$ | $(x, y)$ | 24900 | 24100 | 25200 | 22500 |
| $e_g(d_\pi) \rightarrow b_{2u}(\pi^*)$ | $(x, y)$ | 35600 | 27000 | 36000 | 25300 |
| $e_g(d_\pi) \rightarrow a_{2u}(\pi^*)$ | $(x, y)$ | — | 31900 | — | 30100 |

[a] Only allowed transitions with orbital energy differences of less than 45000 $cm^{-1}$ were included in the table.

Table 5 indicates that the $e_g(d_\pi) \rightarrow b_{1u}(\pi^*)$ transition could possibly also be observed in Ni and Co porphyrins, although with a decreased intensity. The experimental vapor spectra of Co and Ni octaethyl [63] and tetraphenyl [64] porphins do not preclude this possibility. In the 30000 to 40000 $cm^{-1}$ region of the Co and Ni TPP's there seems to be an underlying band which is not present in Cu, Zn, and MgTPP.

The energy of NiPc and NiTAP were calculated for a wide range of skeletal geometries and Ni–$N_{10}$ bond distances [45]. The results demonstrate that TAP is a good model for Pc since geometry changes have similar effects on the $d$ orbitals. The $b_{1g}(d_{x^2-y^2})$ orbital energy is very geometry dependent. A point of interest is that for equal Ni–N bond distances, NiTBP and NiP have a higher calculated $b_{1g}(d_{x^2-y^2})$ energy than NiPc and NiTAP. Therefore, the increased ligand field splitting of phthalocyanines relative to porphyrins is not due to substitution of C–H by nitrogens at the bridge positions, but to a decrease in the metal-nitrogen bond distance.

The energy of the $Np_\sigma$ and $\pi$ orbitals is essentially unaffected by changes in the Ni–N distance but is dependent on skeletal geometry. For example, $e_g(\pi^*)$ decreases by $\sim 0.2$ eV when the TBP geometry is used for NiPc.

As expected, the amount of metal orbital delocalization increases as the Ni–N distance decreases. The composition of $b_{2g}(d_{xy})$ and $b_{2g}^*(d_{xy})$ is especially susceptible to geometry changes. The composition of these orbitals would be very sensitive to ring substitutents rather than to axial ligands.

Our calculations clearly indicate NiPc and NiTAP to be diamagnetic with $b_{2g}(d_{xy}) < e_g(d_\pi) < a_{1g}(d_{z^2}) < b_{2g}^*(d_{xy}) \ll b_{1g}(d_{x^2-y^2})$ (see Fig. 4). The calculated energy gap between $a_{1g}(d_{z^2})$ and $b_{1g}(d_{x^2-y^2})$ is strongly dependent on the Ni–N distance; e.g., it decreases from 3.84 to 2.52 eV as the Ni–N distance increases from 1.83 to 1.96 Å.

One would like to use this result to explain why NiPc shows no tendency to form paramagnetic six coordinate derivatives [13] while nickel porphyrins do form high spin complexes with nitrogen bases [65]. To test this point a calculation was made on a NiTAP dipyridine octahedral complex. The two pyridines raise the energy of $d_{z^2}$ by 2.75 eV and $d_{x^2-y^2}$ by $\sim 0.13$ eV. This result does suggest that NiTAP (and NiPc) would be paramagnetic in the presence of fifth and sixth ligands. That such octahedral coordination is not formed may be due to the small size of the Pc and TAP rings. It is well known that high spin Ni(II)

complexes normally have Ni–N bond distances greater than 2.0 Å. In order to accommodate a high spin Ni(II), the porphyrin ligand can expand its hole size, while for phthalocyanine, such an expansion is impossible. The geometric explanation for lack of formation of pyridine complexes is further supported by the higher positive charge in NiPc compared to NiP – which would tend to favor complex formation.

### *D.* Co

Fig. 4 shows the MO energy levels of Co in comparison with Ni. The major differences from Ni are the shift of the *d* levels to somewhat higher energy – particularly $b_{1g}(d_{x^2-y^2})$ – and the unpaired electron in orbital $a_{1g}(d_{z^2})$. However, our results for CoPc (Co–N distance = 1.90 Å) clearly indicate that the odd electron should go in the $b^*_{2g}(d_{xy})$ orbital. Unfortunately, this does not agree with the conclusion drawn from studies on the magnetic properties [59, 66] and ESR [67, 68] of CoPc. All studies seem to agree that the odd electron is in $d_{z^2}$, in accord with the observation that the ESR of CoPc is solvent dependent while CuPc is not [59, 67]. The abnormal temperature dependence of the magnetic susceptibility of CoPc [59] suggests that $^2E_g$ and $^2B_{2g}$ mix in with the $^2A_{1g}$ ground state.

The calculated $b^*_{2g}(d_{xy}) - a_{1g}(d_{z^2})$ energy gap is not very sensitive to changes in the Co–N distance. Increasing this distance from 1.87 to 1.96 Å does not change the energy separation by more than 0.04 eV. In the crystal, however, one has *N* atoms of parallel molecules lying above and below the molecular plane ~3.4 Å from the metal atom [34]. This will tend to raise the energy of $d_{z^2}$ relative to $d_{xy}$, thus approaching the experimental result. The energy of the $d_{z^2}$ orbital is very sensitive to the presence of ligands; e.g., placing one pyridine 2.0 Å above the plane of CoTAP raises the $d_{z^2}$ energy by ~1.5 eV. However, the odd electron in $d_{z^2}$ actually prevents the close association of any ligands [13].

As for allowed bands in the near UV, CoPc has the same possibilities as NiPc, as shown in Table 5. One extra band is observed [12]. Since the CoPc transitions are generally calculated to be red shifted with respect to NiPc, it may be that some are buried under the Soret band. The hole in $a_{1g}(d_{z^2})$ allows for low energy *z* polarized transitions $a_{2u}(\pi) \rightarrow a_{1g}(d_{z^2})$. This may be observable in solid near *ir* absorption. Also low energy *dd* transitions are possible and would provide pathways for radiationless decay.

### *E.* Fe

The MO diagram for FePc and FeTAP is given in Fig. 5. For FeTAP Fig. 5 also shows a calculation with a shortened $Fe-N_{10}$ distance, the only effect being to raise $b_{1g}(d_{x^2-y^2})$. Consistent with the high energy of this orbital, all investigators save one [69] conclude the spin is $S = 1$. This can be compared to Fe(II) TPP with no ligands, which is clearly high spin [70]. High spin requires a substantial lowering of $b_{1g}(d_{x^2-y^2})$ in porphin. We believe the principal cause of this difference is the larger size of the $Fe-N_{10}$ distance. In Fe(II) porphin the energy of $b_{1g}(d_{x^2-y^2})$ is ~ −8.4 eV for a planar Fe–N distance of 2.05 Å while in Pc and TAP the energy of this orbital goes from −8.0 to −7.7 eV as the Fe–N distance decreases from 1.99 to 1.95 Å (Fig. 5).

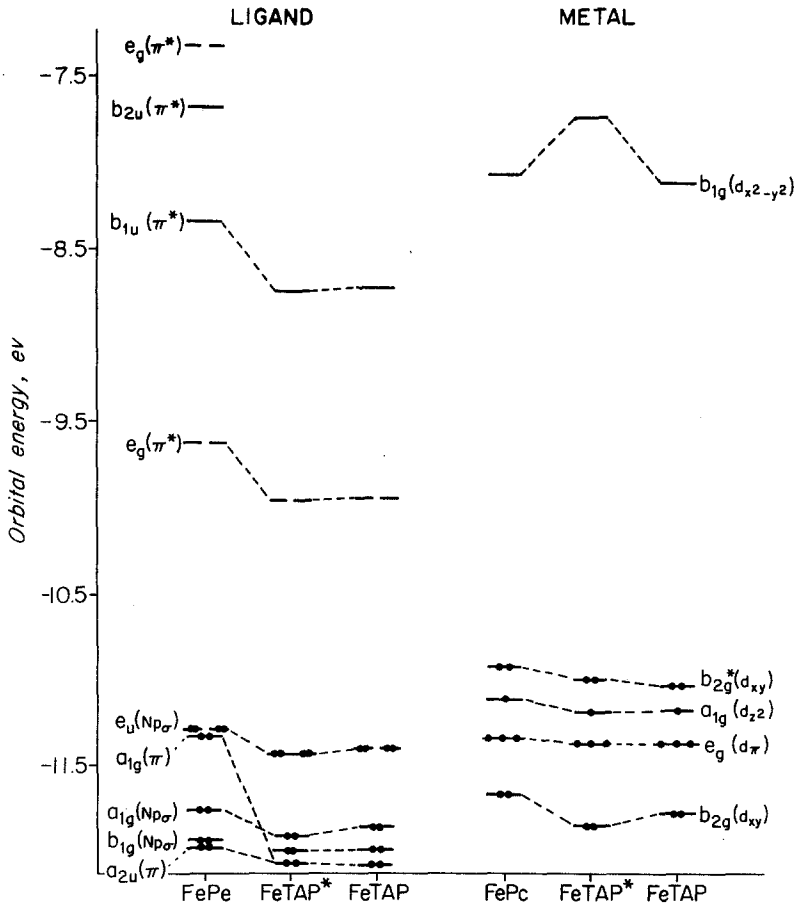


Fig. 5. Top filled and lowest empty ligand and metal MO's of FePc and FeTAP. For FeTAP* the Fe–$N_{10}$ distance was decreased to 1.95 Å. No fifth or sixth ligand on metal

There is some disagreement over the FePc ground state configuration. Dale *et al.* [71] claim a $^3E_g$ ground state while Barraclough *et al.* [72] interpret the magnetic susceptibility and anisotropy data as implying a $^3B_{2g}$ ground state. We predict one odd electron in $a_{1g}(d_{z^2})$ and one in $b_{2g}^*(d_{xy})$, although in Fig. 5 we show one odd electron in $e_g(d_\pi)$ and one in $a_g(d_{z^2})$.

From results of Paper VIII [3] it is clear that raising Fe(II) out of the plane by $\sim 0.49$ Å will make Fe(II) porphin high spin. Since the radius of the phthalocyanine ring is at least 0.05 Å smaller than the corresponding porphyrin, in order to make FePc high spin, the Fe will have to be brought out considerably farther than 0.49 Å. This will weaken the Fe–N bonds considerably, thus making high spin FePc energetically unfavorable. We did calculations on FeTAP-dipyridine which clearly indicate this molecule to be diamagnetic in agreement with experimental measurements [59, 72].

The opening of a hole in $e_g(d_\pi)$ in Fe (and similarly for Mn) opens the possibility for low energy charge transfer transitions $a_{1u}(\pi)$ or $a_{2u}(\pi) \rightarrow e_g(d_\pi)$. These

are $(x, y)$ polarized and may possibly be easily observed in the near IR. Finally we note that with a pyridine ligand we find a possible $b_{2g}(d_\pi) \rightarrow b_{3u}(2p_x^*)$ [$D_{2h}$ notation] charge transfer transition. The $b_{2g}(d_\pi)$ is $\sim 80\%$ localized on the metal while $b_{3u}(2p_x^*)$ is $\sim 98\%$ localized on pyridine. The orbital energy difference is about $22\,500\,\mathrm{cm}^{-1}$ which agrees amazingly well with the charge transfer transition found by Dale [73] in FePc $(\text{pyridine})_2$ at $24\,100\,\mathrm{cm}^{-1}$. Kobayashi and Yanagawa [70] assigned the band at $21\,000\,\mathrm{cm}^{-1}$ in Fe(II)TPP $(\text{pyridine})_2$ to charge transfer from iron to pyridine. As a result of our calculation this assignment seems entirely reasonable.

## F. Mn

MnPc again demonstrates the difference between porphyrins and phthalocyanines. MnPc forms an intermediate-spin, $S = 3/2$, four coordinate complex [59, 72], while Mn porphyrins form a high-spin complex that is most likely five-coordinate and non-planar [74]. Our calculated results for MnPc (Fig. 6) are

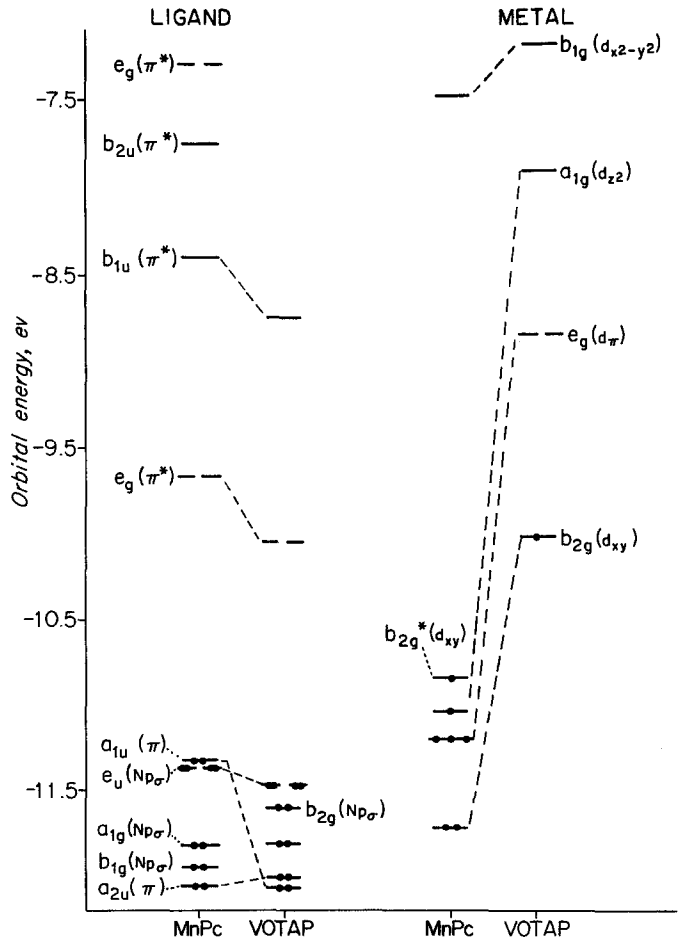


Fig. 6. Top filled and lowest empty ligand and metal MO's of MnPc and VOTAP

again unambiguous. An $e_g(d_\pi)^3\, a_{1g}(d_{z^2})\, b_{2g}^*(d_{xy})$ ground state is indicated. The magnetic moment of MnPc being larger than the spin only value implies that there is a mixing of the ground and excited spin states [72]. Barraclough *et al.* [72] prefer a $d_{xy}{}^2 d_\pi{}^2 d_{z^2}$ ground state with mixing coming from the $d_\pi^3 d_{xy} d_{z^2}$ state.

## G. VO

The MO diagram for VOTAP is given in Fig. 6. We find the odd electron in $d_{xy}$. Because of its relatively high energy, this orbital does not interact with the ring $b_{2g}(Np_\sigma)$ to give $b_{2g}^*(d_{xy})$ and $b_{2g}(d_{xy})$, and we calculate it to be 87% $d_{xy}$ in characters. (See Table 4.) There is some disagreement among the experimentalists as to how pure it is. Assour, Goldmacher, and Harrison [75] concluded it was relatively pure $d_{xy}$ on the basis of lack of nitrogen hyperfine splitting. A similar conclusion had been reached by Kivelson and Lee [76] for VO tetraphenylporphin. More recently Sato and Kwan [77] report nitrogen superhyperfine structure in VOPc and Guzy *et al.* [78] deduce only 73% occupancy.

Zerner and Gouterman [2] identified the 42000 to 50000 $cm^{-1}$ bands observed in vanadyl compounds with a charge transfer transition from oxygen to the unfilled metal orbitals ($d_\pi$ or $d_{z^2}$). In VOTAP we also have the possibility of such transitions. We thus identify the extra band observed by Edwards in VOPc at 48100 $cm^{-1}$ with these charge transitions.

## H. Electronic Populations

Tables 6 and 7 present the results of a Mulliken population analysis for various metal complexes of Pc and TAP. It would be useful to compare these results with those obtained by Zerner and Gouterman for porphyrins [1–5]. Except for Mn, all metals have a greater net positive charge in phthalocyanines. This result is also found if equal bond lengths are used for the phthalocyanine and porphyrin calculations. Except for the reversal of Ni and Cu our metal net charges, Mg > Zn > Co > Cu > Ni > Fe > Mn, follow those in porphyrin.

Charge densities can be somewhat related to stability. The stability of porphyrin derived from consideration of displacement reactions, dissociation reactions, and electronic spectral data is Ni > Co > Cu > Zn > Mg [79]. Thus, the order of increased stability corresponds to a decrease in the ionic character of the metal-nitrogen bond [1]. However, metal phthalocyanines are considerably more stable than the corresponding porphyrin, yet the ionic character of the metal-nitrogen bond is greater in phthalocyanines. Thus predictions about stability involve geometric as well as electronic consideration.

Table 6 shows a slightly greater negative charge on the bridged compared to the central nitrogens. However, their difference is rather small. This contrasts to the far larger difference in charge we have calculated for the three types of nitrogen atoms in $H_2Pc$ with a bonded structure [7]. Zeller and Hayes [80] have recently reported on the X-ray photoelectron spectra of the N 1*s* electron in $H_2Pc$ and CuPc. The broad line observed for $H_2Pc$ and sharp line observed for CuPc agree qualitatively with our calculated charge densities.

Finally we should note that the charge density on any atom does not change more than 0.01 as the geometry is varied.

Table 6. Electronic population of phthalocyanines[a]

A. Total ligand population

| Atom | Mg | Zn | Cu | Ni | Co | Fe | Mn | SCF[a] |
|---|---|---|---|---|---|---|---|---|
| $N_{10}$ | 5.169 | 5.149 | 5.151 | 5.141 | 5.148 | 5.120 | 5.126 | 1.605 |
| $C_{11}$ | 3.932 | 3.924 | 3.918 | 3.926 | 3.927 | 3.924 | 3.918 | 0.834 |
| $C_{12}$ | 4.006 | 4.001 | 3.999 | 3.996 | 3.997 | 3.995 | 3.993 | 1.016 |
| $C_{13}$ | 4.029 | 4.035 | 4.032 | 4.031 | 4.031 | 4.031 | 4.026 | 0.981 |
| $C_{14}$ | 4.042 | 4.042 | 4.041 | 4.039 | 4.041 | 4.039 | 4.039 | 0.998 |
| $N_\alpha$ | 5.196 | 5.188 | 5.196 | 5.184 | 5.179 | 5.198 | 5.178 | 1.238 |
| $H_{13}$[a] | 0.941 | 0.940 | 0.938 | 0.939 | 0.940 | 0.939 | 0.939 | |
| $H_{14}$[a] | 0.946 | 0.946 | 0.941 | 0.945 | 0.945 | 0.945 | 0.944 | |
| Pc[b] | −0.630 | −0.452 | −0.334 | −0.315 | −0.359 | −0.249 | −0.101 | |

B. Metal population

| | 3*d* | 4*s* | 4*p* | Total | Net | Porphin[c] |
|---|---|---|---|---|---|---|
| Mg[d] | | 0.517 | 0.853 | 1.370 | +0.630 | +0.572 |
| Zn | 9.986 | 0.648 | 0.914 | 11.548 | +0.452 | +0.401 |
| Cu | 9.669 | 0.466 | 0.531 | 10.666 | +0.334 | +0.281 |
| Ni | 8.739 | 0.439 | 0.507 | 9.685 | +0.315 | +0.301 |
| Co | 7.718 | 0.381 | 0.542 | 8.641 | +0.359 | +0.342 |
| Fe | 7.136 | 0.301 | 0.314 | 7.751 | +0.249 | +0.226 |
| Mn | 6.357 | 0.352 | 0.190 | 6.899 | +0.101 | +0.111 |

[a] SCMO-PPP $\pi$ electron results, Refs. [19, 20].
[b] Net charge on ligand given.
[c] See Refs. [1–5].
[d] Population of 3*s* and 3*p* given.

Table 7. Electronic population of tetrazaporphins[a]

A. Total ligand population

| Atom | Mg | Zn | Cu | Ni | Co | Fe | VO | SCF |
|---|---|---|---|---|---|---|---|---|
| $N_{10}$ | 5.173 | 5.164 | 5.164 | 5.147 | 5.152 | 5.135 | 5.133 | 1.603 |
| $C_{11}$ | 3.929 | 3.914 | 3.906 | 3.925 | 3.927 | 3.921 | 3.916 | 0.844 |
| $C_{12}$ | 4.041 | 4.035 | 4.037 | 4.027 | 4.029 | 4.026 | 4.025 | 1.003 |
| $N_\alpha$ | 5.180 | 5.179 | 5.178 | 5.171 | 5.168 | 5.174 | 5.169 | 1.200 |
| $H_{12}$[a] | 0.936 | 0.936 | 0.927 | 0.929 | 0.930 | 0.930 | 0.930 | |
| TAP | −0.657 | −0.454 | −0.332 | −0.315 | −0.366 | −0.259 | −0.489 | |

B. Metal population

| | 3*d* | 4*s* | 4*p* | Total | Net |
|---|---|---|---|---|---|
| Mg | | 0.511 | 0.832 | 1.343 | +0.657 |
| Zn | 9.987 | 0.911 | 0.648 | 11.546 | +0.454 |
| Cu | 9.664 | 0.469 | 0.535 | 10.668 | +0.332 |
| Ni | 8.725 | 0.443 | 0.517 | 9.685 | +0.315 |
| Co | 7.691 | 0.386 | 0.557 | 8.634 | +0.366 |
| Fe | 7.113 | 0.303 | 0.324 | 7.741 | +0.259 |
| VO | 3.720 | 0.288 | 0.503 | 4.511 | +0.484 |

[a] For additional detail see footnotes to Table 6.

## Summary

These calculations were undertaken with the hope of elucidating some of the differences between porphyrins and phthalocyanines. We discussed the following points:

(1) A detailed literature investigation into phthalocyanine crystal structure indicates that the radius of the metal phthalocyanine ring is on the average 0.065 Å smaller than the corresponding porphyrin.

(2) The extra UV bands in NiPc and CoPc are suggested to be due to $d_\pi \rightarrow \pi^*$ transitions. One of these transitions is also expected to be observed in Ni and Co porphyrin.

(3) Phthalocyanines and tetrazaporphin are found to have low lying $n \rightarrow \pi^*$ transitions which are probably responsible for the diffuseness of the Soret band.

(4) The $b_{2g}(Np_\sigma)$ orbital of the phthalocyanine and tetrazaporphin ligand mixes with $b_{2g}(d_{xy})$ of Ni, Co, Fe, and Mn to form a lower energy $b_{2g}(d_{xy})$ and a higher energy $b^*_{2g}(d_{xy})$.

(5) The ordering of the $d$ orbitals derived from these calculations differ somewhat from those obtained from ESR and magnetic measurements. The $b^*_{2g}(d_{xy})$ orbital is usually higher than $a_g(d_{z^2})$.

(6) The larger ligand field splitting of phthalocyanines compared to porphyrins is mainly due to the smaller ring size. The inability of the Pc ring to expand as much as porphyrin is used to explain why FePc is of intermediate spin and a high spin NiPc (pyridine)$_2$ complex does not form.

(7) FePc (pyridine)$_2$ is clearly diamagnetic with a $d_\pi \rightarrow$ pyridine charge transfer transition around 24000 cm$^{-1}$.

(8) The skeletal geometry is more important in determining the energy of $Np_\sigma$ and $\pi$ orbitals while the Ni–N bond distance is crucial in determining the ligand field splitting.

*Acknowledgements.* This research was supported in part by Public Health Services Grant GM 14292 from the Division of General Medical Sciences.

## References

1. Paper IV: Zerner, M., Gouterman, M.: Theoret. chim. Acta (Berl.) **4**, 44 (1966).
2. Paper V and VI: Zerner, M., Gouterman, M.: Inorg. Chemistry **5**, 1699, 1707 (1966).
3. Paper VIII: Zerner, M., Gouterman, M., Kobayashi, H.: Theoret. chim. Acta (Berl.) **6**, 363 (1966).
4. Zerner, M.: Ph. D. Thesis, Dept. of Chemistry, Harvard University (1966).
5. Paper X: Zerner, M., Gouterman, M.: Theoret. chim. Acta (Berl.) **8**, 26 (1967).
6. Paper XXI: Schaffer, A. M., Gouterman, M.: Theoret. chim. Acta (Berl.) **18**, 1 (1970).
7. Paper XXV: Schaffer, A. M., Gouterman, M.: Theoret. chim. Acta (Berl.) **25**, 62 (1972).
8. Linstead, R. P.: Brit. Assoc. Advancement Sci., Rep. annu. Meeting 465 (1933).
9. Dent, C. E., Linstead, R. P., Lowe, A. R.: J. chem. Soc. (London), (1934), 1027, 1033.
10. Moser, F. H., Thomas, A. L.: Phthalocyanine compounds. New York: Reinhold Publishing Corporation 1963.
11. Paper VII: Eastwood, D., Edwards, L., Gouterman, M., Steinfeld, J.: J. molecular Spectroscopy **20**, 381 (1966).
12. Paper XV: Edwards, L., Gouterman, M.: J. molecular Spectroscopy **33**, 292 (1970).
13. Lever, A. P.: Advances inorg. Chem. Radiochem. **7**, 27 (1965), and references therein.
14. Stern, A., Pruckner, F.: Z. physik. Chem. **178** A, 420 (1937).
15. Linstead, R. P., Whalley, M.: J. chem. Soc. [London], 4839 (1952).

16. Kuhn, H.: J. chem. Physics **17**, 1198 (1949); Fortschr. Chem. org. Naturstoffe [Wien], **17**, 404 (1959); Angew. Chem. **71**, 93 (1959); Chimia [Aarau, Schweiz], **15**, 53 (1961).
17. Basu, S.: Indian J. Physics Proc. Indian Assoc. Cultivat. Sci. **28**, 511 (1954).
18. Forsterling, H. D., Kuhn, H.: Int. J. quant. Chemistry **2**, 413 (1968).
19. Paper III: Weiss, C., Kobayashi, H., Gouterman, M.: J. molecular Spectroscopy **16**, 415 (1965).
20. Paper XXIV: McHugh, A., Gouterman, M., Weiss, C.: Theoret. chim Acta (Berl.) **24**, 346 (1972).
21. Linder, R. E., Rowlands, J. R.: Molecular Physics **21**, 417 (1971).
22. Taube, R.: Z. Chem. **6**, 8 (1966).
23. Ponomarev, D. A., Kubarev, S. I.: Theoret. Exp. Chem. **4**, 318 (1968).
24. Chen, I., Abkowitz, M., Sharp, J. H.: J. chem. Physics **50**, 2237 (1969).
25. Kramer, L. N., Klein, M. P.: Chem. Physics Letters **8**, 183 (1971).
26. Mathur, S. C., Singh, J.: Int. J. quant. Chemistry **6**, 57 (1972).
27. Henriksson, A., Roos, B., Sundbom, M.: Theoret. chim. Acta (Berl.) **27**, 303 (1972).
28. Wilkinson, J. H.: The algebraic eigenvalue problem. Oxford: Oxford University Press 1965.
29. Davidson, E. R.: unpublished.
30. Fleischer, E. B.: Chem. Comm. 105 (1970).
31. Hoard, J. L.: Sciences **174**, 1295 (1971).
32. Robertson, J. M.: J. chem. Soc. [London] **615** (1935); **1195** (1936).
33. Linstead, R. P., Robertson, J. M.: J. chem. Soc. [London] 1736 (1936).
34. Robertson, J. M., Woodward, I.: J. chem. Soc. [London] 219 (1937); 36 (1940).
35. Brown, C. J.: J. chem. Soc. (A) [London] 2494 (1968).
36. Hoskins, B. F., Mason, S. A., White, J. C. B.: Chem. Comm., 554 (1969).
37. Fischer, M., Templeton, D. H., Zalkin, A., Calvin, M.: J. Amer. chem. Soc. **93**, 2622 (1971).
38. Brown, C. J.: J. chem. Soc. (A) [London], 2488 (1968).
39. Vogt, L. H. Jr., Zalkin, A., Templeton, D. H.: Inorg. Chemistry **6**, 1725 (1967).
40. Friedel, M. K., Hoskins, B. F., Martin, R. L., Mason, S. A.: Chem. Comm., 400 (1970).
41. Rogers, D., Osborn, R. S.: Chem. Comm., 840 (1971).
42. Kobayashi, T., Kurokawa, F., Ashida, T., Uyeda, N., Suito, E.: Chem. Comm., 1631 (1971).
43. Kobayashi, T., Ashida, T., Natsu, N., Suito, E., Kakudo, M.: Bull. chem. Soc. Japan **44**, 2095 (1971).
44. D'Addario, A. D.: Diss. Abst. Int. B **32**, 1423 (1971).
45. Schaffer, A. M.: Ph. D. Thesis, Chemistry Department, University of Washington, Seattle (1972).
46. Fielding, P. E., MacKay, A. G.: J. chem. Physics **38**, 2777 (1963).
47. Fielding, P. E., MacKay, A. G.: Austral. J. Chem. **17**, 750 (1964).
48. Schectman, B. H., Spicer, W. E.: J. molecular Spectroscopy **33**, 28 (1970).
49. Day, P., Williams, R. J. P.: J. chem. Physics **42**, 4049 (1965).
50. Day, P., Price, M. G.: J. chem. Soc. (A) [London], 236 (1969).
51. Edwards, L.: Ph. D. Thesis, Committee on Chemical Physics, Harvard University (1969).
52. Baguley, M. E., France, H., Linstead, R. P., Whalley, M.: J. chem. Soc. [London], 3521 (1955).
53. Vincett, P. S., Voigt, E. M., Rieckhoff, K. E.: J. chem. Physics **55**, 4131 (1971).
54. Henriksson, A., Sundbom, M.: Theoret. chim. Acta (Berl.) **27**, 213 (1972).
55. Hockstrasser, R. M., Marzzacco, C.: J. chem. Physics **49**, 971 (1968).
56. Sevchenko, A. N., Shkirman, S. F., Mashenkev, V. A., Solov'ev, K. N.: Soviet Phys – Dokl. **12**, 710 (1968).
57. Harrison, S. E., Assour, J. M.: J. chem. Physics **40**, 365 (1964).
58. Guzy, C. M., Raynor, J. B., Symons, M. C. K.: J. chem. Soc. (A) [London], 2299 (1969).
59. Lever, A. B. P.: J. chem. Soc. [London], 1821 (1965).
60. Martin, R. L., Mitra, S.: Inorg. Chemistry **9**, 182 (1970).
61. Paper XVIII: Eastwood, D., Gouterman, M.: J. molecular Spectroscopy **35**, 359 (1970).
62. Paper XXII: Callis, J. B., Gouterman, M., Jones, Y. M., Henderson, B. H.: J. molecular Spectroscopy **39**, 410 (1971).
63. Paper XVI: Edwards, L., Gouterman, M., Dolphin, D. H.: J. molecular Spectroscopy **35**, 90 (1970).
64. Paper XVII: Edwards, L., Dolphin, D. H., Gouterman, M., Adler, A. D.: J. molecular Spectroscopy **38**, 16 (1971).
65. McLees, B. D., Caughey, W. S.: Biochemistry **7**, 642 (1968).
66. Martin, R. L., Mitra, S.: Chem. Physics Letters **3**, 183 (1969).
67. Assour, J. M., Kahn, W. K.: J. Amer. chem. Soc. **87**, 207 (1965).

68. Rollman, L. D., Chan, S. I.: Inorg. Chemistry **10**, 1972 (1971).
69. Dizsi, I., Balázs, A., Molnár, B., Gorobshenko, V. D., Lukashevich, I. I.: J. inorg. nuclear Chem. **31**, 1661 (1969).
70. Kobayashi, T., Yanagawa, Y.: Bull. chem. Soc. Japan **45**, 450 (1972).
71. Dale, B. W., Williams, R. J. P., Johnson, C. E., Thorp, T. L.: J. chem. Physics **49**, 3441 (1965).
72. Barraclough, C. G., Martin, R. L., Mitra, S., Sherwood, R. C.: J. chem. Physics **53**, 1638, 1643 (1970).
73. Dale, B. W.: Trans. Faraday Soc. **65**, 331 (1969).
74. Boucher, L.: Coord. Chem. Rev. **7**, 289 (1972).
75. Assour, J. M., Goldmacher, J., Harrison, S. E.: J. chem. Physics **43**, 159 (1965).
76. Kivelson, D., Lee, S.-K.: J. chem. Physics **41**, 1896 (1964).
77. Sato, M., Kwan, T.: J. chem. Physics **50**, 558 (1969).
78. Guzy, C. M., Raynor, J. B., Stodulski, L. P., Symons, M. C. R.: J. chem. Soc. (A) [London], 997 (1969).
79. Boucher, L. J., Katz, J. J.: J. Amer. chem. Soc. **89**, 1340 (1967).
80. Zeller, M. V., Hayes, R. G.: submitted for publication.

Dr. Arnold M. Schaffer
Department of Chemistry
University of Houston
Houston, Texas 77004, USA